

## Selectively Thermally Cleavable Fluorinated Side Chain Block Copolymers: Surface Chemistry and Surface Properties

Alexander Böker,<sup>‡</sup> Karsten Reihs,<sup>\*,§</sup> Jianguo Wang,<sup>⊥</sup> Reimund Stadler,<sup>†,‡</sup> and Christopher K. Ober<sup>⊥</sup>

*Makromolekulare Chemie II, Universität Bayreuth, Universitätsstrasse 30, 95440 Bayreuth, Germany, Zentrale Forschung, Bayer AG, 51368 Leverkusen, Germany, and Materials Science & Engineering, Cornell University, 327 Bard Hall, Ithaca, New York 14853-1501*

*Received May 26, 1999; Revised Manuscript Received September 7, 1999*

**ABSTRACT:** A series of monodisperse poly(styrene-*b*-isoprene[*-g*-perfluoroacyl]) block copolymers was synthesized by sequential anionic polymerization of styrene and isoprene. The perfluorinated ester side chains were attached to the remaining double bonds of the isoprene block via oxidative hydroboration and esterification of the resulting alcohol by the corresponding perfluorinated acid chloride. Surfaces of the pure polymers or blends in polystyrene exhibit a notable fractional surface excess of the perfluorinated side chains within the uppermost 100 Å depending on the surface preparation and the block copolymer composition. Thus, these surfaces are highly hydrophobic having advancing water contact angles of up to 122°. When samples are heated to 340 °C, the perfluorinated side chains can be selectively cleaved off by a thermal ester cleavage, leaving the backbone of the polymer completely intact. As a result, the hydrophobicity of the resulting poly(styrene-*b*-isoprene) polymer surface is reversed to an advancing water contact angle < 90°. The selective thermal ester cleavage in combination with a subsequent chemical surface derivatization may have the potential to selectively change the surface functionality. If the thermal cleavage is done locally, patterning of the surface functionality seems possible.

### Introduction

A common approach to develop low surface energy surface uses fluorinated groups in a polymer.<sup>1,2</sup> The resulting fluorine-rich surfaces are highly hydro- and oleophobic<sup>1,2</sup> and have been widely studied as materials for low surface energy coatings.<sup>3,4</sup> Blending of fluorinated block copolymers with homopolymers is well-known to lead to immense changes of the surface properties—namely its hydrophobicity—of the homopolymer as the fluorinated block segregates toward the polymer/air interface, thus considerably decreasing the surface energy.<sup>5–7</sup>

Our aim in this study was to develop polymers with fluorinated side chains, i.e., perfluorinated alkyl groups in order to produce extremely low energy surfaces. Furthermore, we demonstrate that the fluorinated side chains can be cleaved by a defined and selective thermal reaction that leaves the backbone of the polymer completely intact. Upon thermal cleavage, the absence of fluorinated side chains leads to a substantial increase of the surface energy. Likewise, the defined reaction product after thermal cleavage offers the potential for chemical surface derivatization, thus suggesting a scheme to change the surface chemistry and subsequently its surface properties in a very controlled manner. Since the thermal cleavage can be carried out locally, the surface properties can be patterned accordingly. Hydrophobic patterns that can be applied to printing plates using aqueous inks are just a base example for the broad field of patterned chemical surface functionalities.

The use of fluorinated side chain esters provides two main advantages. First, the low surface energy property

of the fluorocarbon chain brings the ester functionality close to the surface in the upper layer of the polymer film. The immiscibility of PS and the fluorinated isoprene block is known to lead to phase separation, yielding a surface that mostly consists of fluorocarbon groups. Second, the reactive fluorinated ester group allows to cleave these ester side chains by pyrolysis or hydrolysis. Hence, the surface can be functionalized with double bonds or hydroxyl groups, respectively. The use of weak ester bonds refers to techniques already applied in photoresist chemistry.<sup>8</sup> Similar poly(styrene-*b*-butadiene) copolymers having perfluorooctanoic ester side chains were previously reported by Antonietti et al.<sup>25</sup> for the construction of ultralow energy surfaces. In addition, this study presents a detailed investigation of the thermal stability of such perfluoroacyl side chains.

We synthesized monodisperse poly(styrene-*b*-isoprene[*-g*-perfluoroacyl]) block copolymers based on poly(styrene-*b*-1,2/3,4-isoprene) followed by grafting the isoprene units with perfluorinated chains. Grafting was achieved by an oxidative hydroboration and subsequent esterification of the resulting alcohol with the corresponding perfluorinated acid chloride. By controlling the block ratio and the lengths of the side chains, we investigated the influence of the chemical structure on the surface properties using surface-sensitive characterization techniques.

### Experimental Section

The base polymers were synthesized by anionic polymerization and final modification by quantitative hydroboration reaction under inert nitrogen atmosphere (see Scheme 1). The isolation of the resulting products includes precipitation in a basic solution intending to eliminate side reactions that might lead to cross-linking. Gel permeation chromatography (GPC) proved that the monodispersity has been retained after the hydroboration and final oxidation. These reactions quantitatively converted the pendant vinyl groups (1,2- and 3,4-

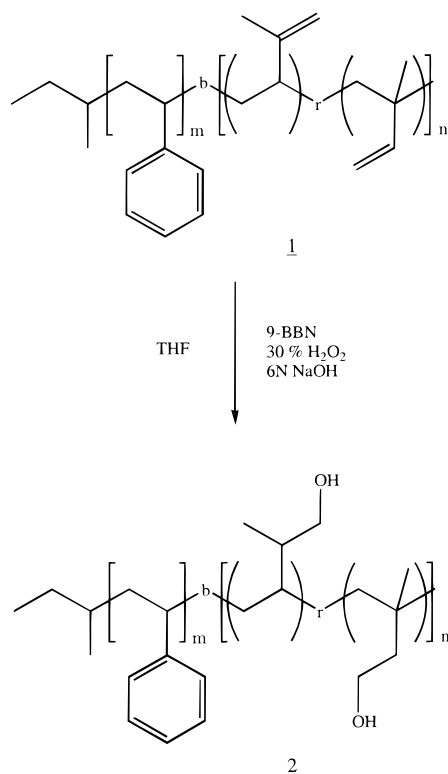
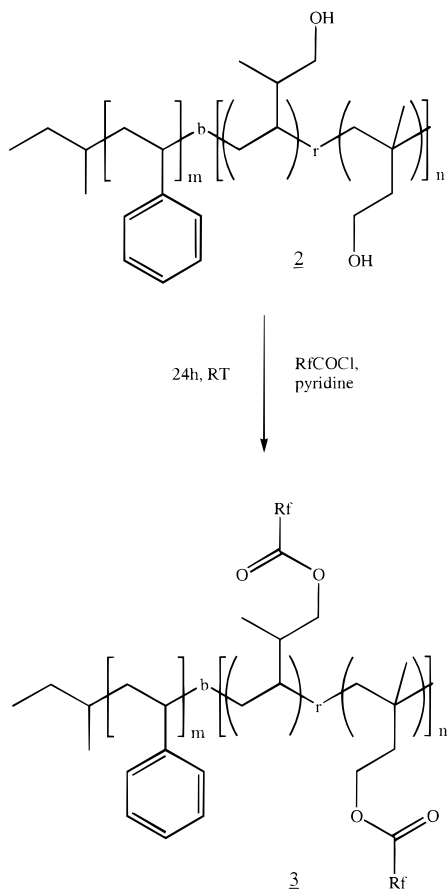
\* Corresponding author.

† Deceased.

‡ Universität Bayreuth.

§ Bayer AG.

⊥ Cornell University.

**Scheme 1. Hydroboration of Poly(styrene-*b*-isoprene)****Scheme 2. Attachment of Fluorinated Ester Side Chains (R<sub>f</sub> Represents the Aliphatic Fluorocarbon Chain, e.g., (CF<sub>2</sub>)<sub>6</sub>CF<sub>3</sub> for Perfluoroheptyl Side Chains, F7)**

isoprene) to hydroxyl groups. The attachment of the fluorinated ester side chains was accomplished by reaction between

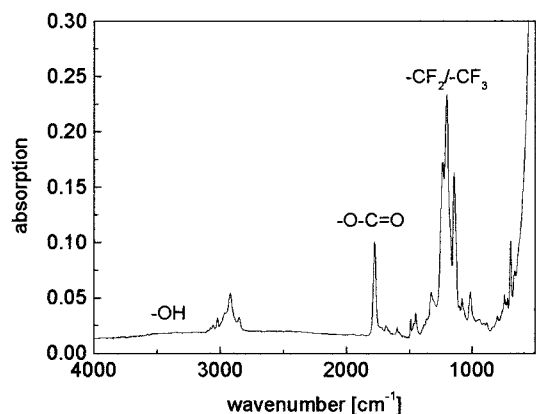


**Figure 1.** FT-IR spectrum of the fluorinated side chain block copolymer SI-26/7-F7.

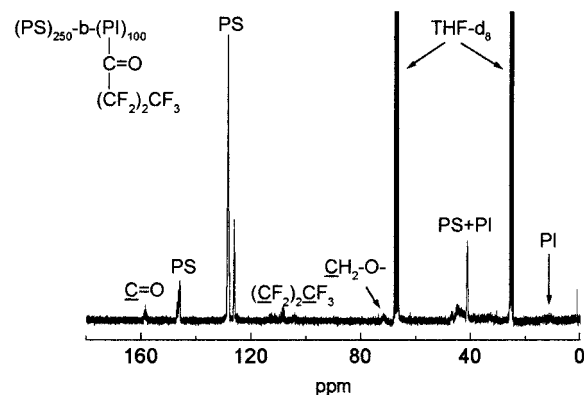


**Figure 2.** <sup>13</sup>C NMR spectrum of the fluorinated side chain block copolymer SI-26/7-F3.

the perfluorinated acid chloride and the hydroxylated block copolymer (see Scheme 2). The yield of that reaction was close to 100% as confirmed by FT-IR measurements. The spectra revealed no residual hydroxyl groups after the esterification reaction as shown in Figure 1. A typical <sup>13</sup>C NMR spectrum and the peak assignment are given in Figure 2. The polyisoprene block consists of approximately 40% 1,2- and 60% 3,4-isomers as revealed by FT-IR and <sup>1</sup>H NMR measurements (see Figure 3). The perfluorinated block copolymers were synthesized to give several series of polymers with a constant degree of polymerization in each series that only differ in the length of the perfluorinated ester side chain as shown in Table 1.

**Solvents and Starting Materials.** Unless noted, all chemicals except perfluorononanoyl chloride (Lancaster, PCR) were purchased from Aldrich and used without further purification. The monomers were purified by standard methods. Styrene was stirred twice over calcium hydride for 24 h, and finally, after overnight treatment with MgBu<sub>2</sub> (bright yellowish color), it has been condensed into an ampule and set under a positive pressure of nitrogen for storage. Isoprene was treated in a comparable manner with MgBu<sub>2</sub> (light yellow color). After condensation into a cold trap, *n*-butyllithium was added and the mixture was stirred for 2 h while it was cooled with ice. Finally, isoprene was condensed into an ampule and set under positive nitrogen pressure for storage. The solvent tetrahydrofuran (THF) was freshly distilled from sodium/benzophenone after refluxing for 2 days and was titrated with 20 mL *sec*-BuLi/liter prior to the polymerization.

**Synthesis of Perfluorodecanoyl Chloride (F9-Chloride).** A 5 g (9.73 mmol) sample of perfluorodecanoic acid was mixed with 5 mL of thionyl chloride and 5 drops of pyridine. The mixture was heated to 60 °C, and the reaction was allowed to proceed overnight. The reaction mixture phase separated upon cooling to room temperature. The lower phase mainly contained perfluorinated acid chloride, which was purified by

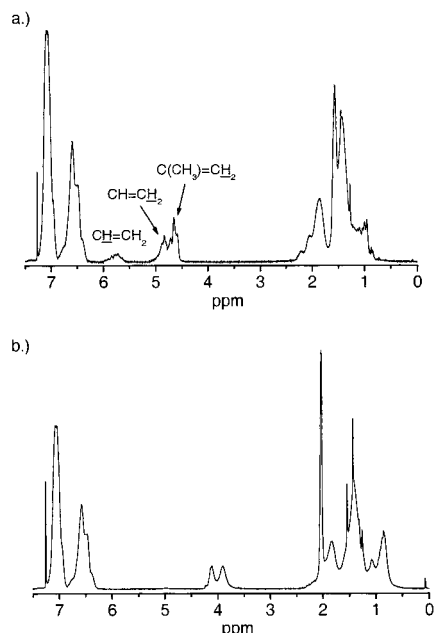


**Figure 3.**  $^1\text{H}$  NMR spectra of starting P(S-b-I) block copolymer SI-46/11 before (a) and after (b) hydroboration. The hydroxylated block was capped with acetyl chloride to increase solubility in  $\text{CDCl}_3$ .

reduced pressure distillation after separation from the upper thionyl chloride containing layer.

Yield: 3.5 g (70%) of white waxy crystals: bp (30 mmHg): 78–80 °C (Lit.<sup>9</sup> bp (747 mmHg): 170–172 °C). IR (film on NaCl plate),  $\tilde{\nu}$  ( $\text{cm}^{-1}$ ): 1803 (acid chloride carbonyl), 1251, 1216, 1151, 1020, 923, 668.

**Copolymerization of Styrene and Isoprene (1).** The basic polymers were synthesized by sequential anionic polymerization of styrene and isoprene at  $-78$  °C (cryostat) in THF as solvent under high purity nitrogen. The synthesis of poly(styrene-*b*-isoprene) with, e.g., 20 wt % isoprene was carried out as follows: 0.533 mL of a solution of 1.3 mol/L *sec*-BuLi in *n*-hexane was added to 1.5 L of freshly distilled and titrated THF, and then 36 g (0.346 mol) of styrene was added (deep orange-red color). The reaction was held at  $-78$  °C for 1 h before 36.38 g (0.535 mol, 4-fold excess) of isoprene was injected into the reaction mixture whereby the color changed to light yellow. The reaction was allowed to proceed for another 4 days at  $-78$  °C and was finally terminated by injecting 1 mL of degassed anhydrous methanol after the product was monitored by  $^1\text{H}$  NMR. Finally, the polymer was precipitated into 5 L of 2-propanol and dried under vacuum at room temperature.

Yield: 41 g (90%) SI-46/11, 25% conversion of isoprene.  $^1\text{H}$  NMR ( $\text{CDCl}_3$ , 250 MHz),  $\delta$  (ppm): 0.8–2.3 (hydrocarbon backbone and aliphatic isoprene units), 4.5–4.8 ( $\text{C}(\text{CH}_3)=\text{CH}_2$ ), 4.8–5.1 ( $\text{CH}=\text{CH}_2$ ), 5.6–6.0 ( $\text{CH}=\text{CH}_2$ ), 6.3–7.2 (aromatic polystyrene units). IR (film on NaCl plate),  $\tilde{\nu}$  ( $\text{cm}^{-1}$ ): 3065, 1641, 1600, 1492, 1452, 1027, 996/910 (1,2 double bond), 886 (3,4 double bond), 756, 698.

**Hydroboration of the Poly(1,2- and 3,4-isoprene) Block (2).** The reaction was performed according to reported procedures<sup>10,11</sup> using 9-bora[3.3.1]bicyclononane (9-BBN) as a known hydroboration agent of unsaturated polymers.<sup>12</sup> A 10 g sample of SI-46/11 (28.1 mmol of  $\text{C}=\text{C}$  groups) was vacuum-dried overnight at room temperature in a 500 mL flask equipped with a Teflon stopcock and a rubber septum before the sample was dissolved in 200 mL of THF (freshly distilled from sodium/benzophenone under nitrogen). The solution was cooled to  $-15$  °C before 70 mL (20% excess) of a 0.5 M solution of 9-bora[3.3.1]bicyclononane in THF was transferred in via a cannula. The solution was stirred for 24 h at room temperature before 1 mL of anhydrous and degassed methanol was injected at  $-25$  °C. After 30 min, 6.4 mL of 6 N NaOH (purged with

nitrogen for 30 min) was added dropwise to the reaction mixture (clear phase separation). After 10 min, 12.8 mL of 30% hydrogen peroxide was injected, and the solution immediately became cloudy and a fine precipitate appeared. After additional 2 h at  $-25$  °C, the solution was allowed to warm to room temperature and after 30 min was heated to 55 °C for 1 h. At this point a white suspension formed. After the mixture was allowed to cool to room temperature, it phase separated again. The aqueous phase was frozen, and the organic layer was poured into 1.8 L of 0.25 M NaOH. The resulting precipitates were stirred overnight in the alkaline environment, transforming the remaining  $\text{H}_3\text{BO}_3$  to  $\text{NaB}(\text{OH})_4$  and removing it from the reaction mixture together with dihydroxycyclooctane in order to prevent the hydroxylated polymer from cross-linking. Further purification included dissolving the precipitate in 100 mL of THF and reprecipitation in mixtures of 600–700 mL of  $\text{MeOH}$ :0.25 M NaOH (1:3, 1:1; v:v). Finally it was washed with water and methanol and dried under vacuum.

Yield: 9.9 g (95%) SI-46/11-OH.  $^1\text{H}$  NMR ( $\text{CDCl}_3$ , 250 MHz),  $\delta$  (ppm): 0.8–2.3 (hydrocarbon backbone and aliphatic isoprene units), 2.1 ( $\text{CH}_3\text{COO}$ ), 3.8–4.2 ( $\text{R}-\text{CH}_2-\text{O}$ ), 6.3–7.2 (aromatic polystyrene units). The hydroxylated block was capped with acetyl chloride to increase solubility in  $\text{CDCl}_3$ . IR (film on NaCl plate),  $\tilde{\nu}$  ( $\text{cm}^{-1}$ ): 3345, 3025, 2925, 1600, 1492, 1452, 1378, 1050.

The synthesis of the polymers with a higher content of hydroxyl groups was similar to SI-46/11-OH. Only the precipitation and isolation was performed slightly different. As those polymers are more polar than SI-46/11-OH, they were redissolved in methanol:THF (2:1, v:v) and washed with pure water after precipitation.

**Attachment of the Perfluorinated Ester Side Chains (3).** The reactions were performed in a similar way, as reported.<sup>13</sup> Only the synthesis of SI-46/11-F7 is described here. All other reactions were carried out in a comparable manner. A 0.5 g sample of polymer SI-46/11-OH (=1.42 mmol of  $-\text{OH}$ ) was dissolved in 15 mL of freshly distilled THF. Then, 3 mL of pyridine and 0.44 mL (0.77 g, 25% excess) of perfluorooctanoyl chloride ( $M = 432.5$  g/mol;  $\rho = 1.744$  g/mL) were added. After 20 h at 45 °C, the reaction was allowed to cool to room temperature and was terminated by adding 1.25 mL of anhydrous  $\text{MeOH}$ . The isolation involved precipitation of the fluorinated polymer in a mixture of 80 mL of  $\text{MeOH}$  and 40 mL of water. The polymer was then dissolved in 10 mL of THF and precipitated three more times. Finally, the polymer was washed with water and dried overnight under vacuum at room temperature.

Yield: 1.1 g (95%) SI-46/11-F7. IR (film on NaCl plate),  $\tilde{\nu}$  ( $\text{cm}^{-1}$ ): 3025, 2925, 1779 (perfluorinated ester carbonyl), 1600, 1492, 1452, 1330, 1207, 1149, 1054, 746. The yield of each attachment reaction was close to 100% as confirmed by FT-IR (no residual  $-\text{OH}$ -groups were detected).

**Sample Preparation.** The polymer films were prepared from 5 wt % solutions of the fluorinated block copolymer or mixtures of the block copolymer and polystyrene in  $\alpha,\alpha,\alpha$ -trifluorotoluene. Thin films (approximately 2000 Å as obtained by atomic force microscopy at an edge of the film) were prepared by spin coating 0.1 mL of the solutions onto a  $1 \times 1$  cm piece of a polished silicon wafer (2000  $\text{s}^{-1}$ , 20 s). Thick films (approximately 5  $\mu\text{m}$ , obtained by scanning electron microscopy of a freeze-fractured sample) were prepared by casting 0.1 mL of the polymer solution into a cylindrical vessel (15 mm diameter) obtained by clamping a glass cylinder onto a polished silicon wafer. A cap with a small orifice allowed for slow solvent evaporation over 12 h. Prior to use, all films were dried overnight under vacuum at room temperature and annealed at 140 °C for 3 h in a vacuum oven.

**Gel Permeation Chromatography (GPC).** GPC measurements were performed using a Waters GPC equipped with dual detectors (RI and UV [ $\lambda = 254$  nm]) and PL-gel columns of 10  $\mu\text{m}$  particle size having  $10^5$ ,  $10^4$ ,  $10^3$ , and  $10^2$  Å pore size. The elution solvent was THF at room temperature with an elution rate of 1 mL/min. Narrow polydispersity polystyrene samples were used as calibration standards.



Table 1. Synthesized Fluorinated Side Chain Block Copolymers

polymer	degree of polymerization (PS:PI)	block ratio (PS:F-PI) [kg/mol]	volume fraction of fluorinated block	$M_w$ (GPC) [kg/mol]	polydispersity
SI-26/7	250:100	25.9:6.9	21.2	35.2	1.02
SI-26/7-F3		25.9:28.2	52.1	41.7	1.03
SI-26/7-F7		25.9:48.2	65.0	micelle: 36 and 560	each monodisperse
SI-26/7-F8		25.9:53.2	67.3	micelle: 33 and 250	each monodisperse
SI-26/7-F9		25.9:58.2	69.2	<i>a</i>	
SI-46/11	440:160	45.6:10.8	19.2	63.6	1.03
SI-46/11-F3		45.6:44.8	49.6	63.7	1.05
SI-46/11-F7		45.6:76.8	62.7	<i>a</i>	
SI-46/11-F8		45.6:84.8	65.0	<i>a</i>	
SI-66/19	640:280	65.9:18.7	22.1	92.5	1.03
SI-66/19-F3		65.9:78.3	54.3	<i>a</i>	
SI-66/19-F7		65.9:134.3	67.1	<i>a</i>	
SI-66/19-F8		65.9:148.3	69.2	<i>a</i>	

<sup>a</sup> No signal could be detected by GPC. The copolymers are abbreviated by their molecular masses of the corresponding blocks: e.g. for SI-26/7-F3,  $M_w$  = 26 kg/mol of styrene,  $M_w$  = 7 kg/mol of isoprene, F3 = perfluorobutyl side chain (none = no side chain, OH = hydroxyl, F7 = perfluorooctanoyl, F8 = perfluorononanoyl, F9 = perfluorodecanoyl).

**FT-Infrared Spectrometry (FT-IR).** FT-IR was carried out using a Bruker EQUINOX 55/S instrument. The samples were thin films cast from THF solution on NaCl crystal plates and dried under vacuum at room temperature. The scan range was 400–4000  $\text{cm}^{-1}$  covered by 128 scans at a resolution of 4  $\text{cm}^{-1}$ .

**<sup>1</sup>H and <sup>13</sup>C NMR Spectra.** <sup>1</sup>H NMR spectra were acquired on a 250 MHz Bruker AC 250 instrument using  $\text{CDCl}_3$  as solvent and tetramethylsilane (TMS) as internal standard. <sup>13</sup>C NMR spectra were acquired at 62.5 MHz using a Bruker AC 250 instrument with  $\text{THF}-d_6$  as solvent.

**Transmission Electron Microscopy (TEM).** The bulk morphology of the perfluorinated side chain block copolymers was examined using TEM. Films (around 1 mm thick) were cast from 5 wt % solutions in toluene and allowed to evaporate slowly for 5 days. The as-cast films were dried for 1 day in a vacuum oven at room temperature followed by annealing at 140 °C for 1 week under vacuum. Thin sections were cut at 140 K using a Reichert-Jung Ultracut E microtome equipped with a diamond knife. To enhance the electron density contrast between areas of the fluorinated and PS blocks, the sections were stained for 5 min in  $\text{RuO}_4$  vapor, which preferentially stains the interface of the PS block and the fluorinated block in these polymers. Bright field TEM was performed using a Zeiss electron microscope (CEM 902) operated at 80 kV.

**X-ray Photoelectron Spectroscopy (XPS).** XPS measurements were performed using a Vacuum Generator instrument (VG-220iXL) using Al K $\alpha$  radiation (1486.6 eV) from a polychromatic source operating at 240 W (12 kV, 20 mA). The electron analyzer was operated in the electromagnetic lens mode at a takeoff angle (angle between the axis of the analyzer and the surface) of 90° using a sampling area of 5 mm in diameter. The chamber pressure was  $10^{-8}$ – $10^{-9}$  mbar during analysis. High-resolution spectra were analyzed using a least-squares curve-fitting program. The peak positions were determined according to previously established binding energies.<sup>14</sup> Deviations to these energies were typically on the order of  $\pm 0.1$  eV. The Gauss–Lorentzian shape ratios of individual lines were fixed at 30% Gaussian. All spectra were referenced to a binding energy of 284.6 eV for C–C/C–H carbon moieties.

Angle-dependent measurements (ADXPS) were performed using the electrostatic lens mode leading to a sufficiently narrow solid angle of electron acceptance and a sampling area of 150  $\mu\text{m}$  in diameter. The takeoff angles were  $\alpha$  = 10, 30, 50, and 90°. Considerable attention was applied to the proper eucentric alignment of the 4-axis sample manipulator for the angle-dependent experiments. The attenuation of photoelectrons due to scattering from subsurface layers was taken into account by the inelastic mean free path  $\lambda$  (IMFP) in an exponential decay law.<sup>15,16</sup> The sampling depth  $d$  used here is defined as  $d = 3\lambda(\sin \alpha)$ , from which 95% of the photoelectrons originate. The IMFP was estimated from known empirical

correlations with the kinetic energy of the photoelectrons.<sup>16</sup> The spectra were measured with 15 scans/region (C 1s, O 1s, F 1s) and 3 scans/angle.

Possible X-ray degradation during the measurements was checked by the atomic percentage of carbon, oxygen, and fluorine of selected polymer samples before and after a subsequent control measurement. They remained the same within the experimental error of XPS (10% relative), which suggests that no significant X-ray induced degradation occurred.

**Static and Dynamic Secondary Ion Mass Spectrometry (sSIMS, dSIMS).** The SIMS spectra were measured, using an IONTOF instrument (ToF–SIMS IV) equipped with three primary ion sources. In the static mode  $\text{Ar}^+$  ions were used as primary ions with a dose density (PIDD) of approximately  $6 \times 10^8$  ions/ $\text{cm}^2$ , an energy of 10 keV (sample current 1 pA), and a sampling area of (100  $\mu\text{m}$ )<sup>2</sup>. The main chamber pressure was below  $5 \times 10^{-9}$  mbar. Depth profiles in the dynamic mode were obtained by sample erosion with  $\text{O}_2^+$  ions (3 keV, 45 nA, PIDD  $\approx 8 \times 10^{17}$  ions/ $\text{cm}^2$ ), producing craters of (200  $\mu\text{m}$ )<sup>2</sup> area. Primary ions used for the intermediate analysis during sample erosion were  $\text{Ga}^+$  ions (20 keV, PIDD  $\approx 1 \times 10^9$  ions/ $\text{cm}^2$ ) covering a sampling area of (100  $\mu\text{m}$ )<sup>2</sup> inside the erosion crater.

**Contact Angles.** Contact angles of spin-coated and annealed (3 h, 140 °C) films were determined using a NRC contact angle goniometer model 100-00 (Ramé-Hart Inc.) at 25 °C. The given contact angles are averages of at least three measurements. The advancing contact angle was measured while the volume of a 4  $\mu\text{L}$  liquid drop was slowly increased using the cannula of a syringe. The receding angle was determined by removing liquid from the droplet while the static contact angle was obtained by using a free drop of liquid of approximately 4  $\mu\text{L}$  on the polymer surface.

**Thermogravimetric Analysis (TGA) and Thermal Desorption Mass Spectrometry (TDMS).** Thermogravimetric analysis was performed on a Perkin-Elmer TGA 7 under nitrogen atmosphere using a heating rate of 5 K/min, starting from room temperature up to 600 °C. The sample weight was approximately 5 mg in all cases. Thermal desorption mass spectrometry was performed using a home-built standard ultrahigh vacuum (UHV) setup consisting of an airlock, UHV preparation chamber, and UHV main chamber with a differentially pumped quadrupole mass spectrometer (Hiden HAL/3F 301C) equipped with a 70 eV electron impact ion source. The thin film samples on polished silicon wafers as substrates were heated with a rate of 5 K/min, starting from room temperature to 600 °C using an electrically heated sample support. Fragments emitted from the sample upon heating were ionized and monitored by their partial pressure using the quadrupole mass spectrometer.

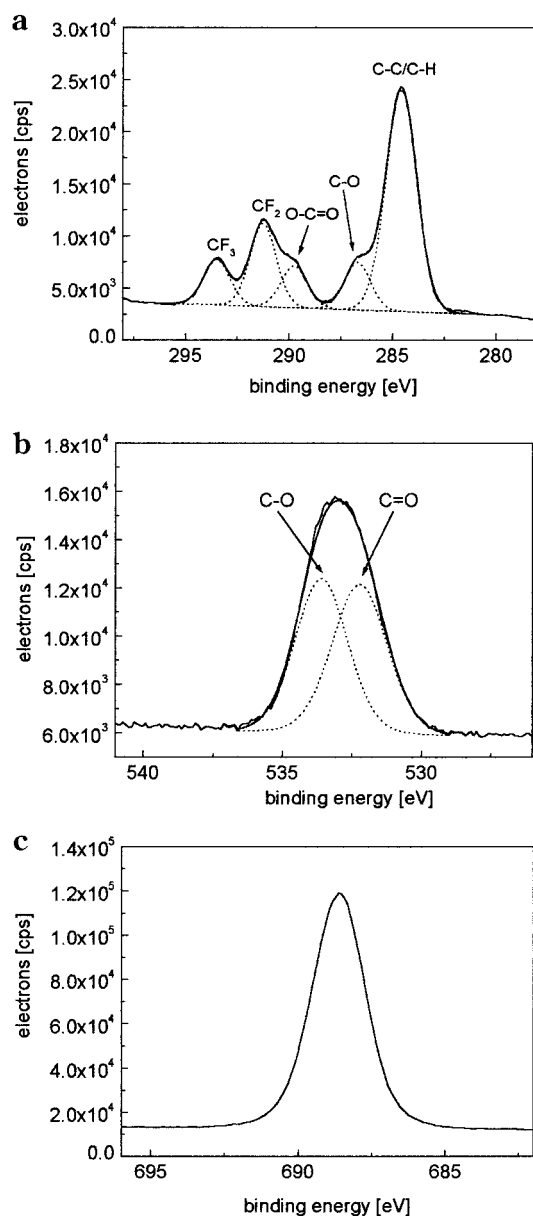


**Figure 4.** XPS spectra for (a) C 1s, (b) O 1s, and (c) F 1s regions of SI-46/11-F3.

## Results and Discussion

**Pure Block Copolymers.** It is a well-understood phenomenon that differences in the surface free energy of the components within a polymer or a polymer system highly influence the surface composition in such a way that the lower surface energy segments reside at the polymer/air interface. As shown by Kramer et al., the magnitude of the surface excess is determined by the surface tensions and the interaction parameter of the segments.<sup>17</sup> As a consequence, in systems with high differences of the surface free energy of the two segments, the chemical composition of the surface area highly differs from the composition of the bulk. Such surface segregation of the low energy fluorinated side chains can also be observed for the block copolymers in this study.

High-resolution XPS spectra with an electron takeoff angle of 90° that corresponds to a sampling depth of approximately 100 Å are shown in Figures 4 and 5 for SI-46/11-F3 and SI-46/11-F8 respectively and are representative for all the analyzed samples. The inter-

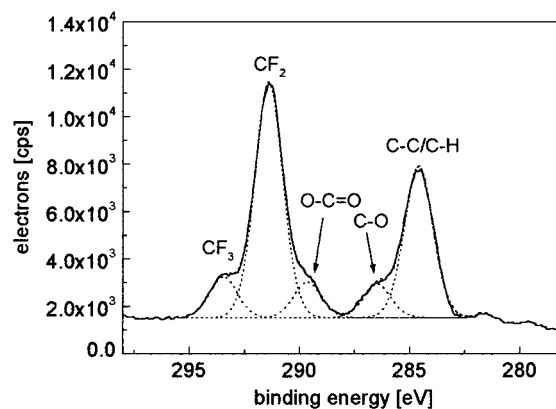


**Figure 5.** XPS C 1s regional scan of SI-46/11-F8.

**Table 2. XPS Peak Assignments and Binding Energies (in eV) of Block Copolymers SI-46/11**

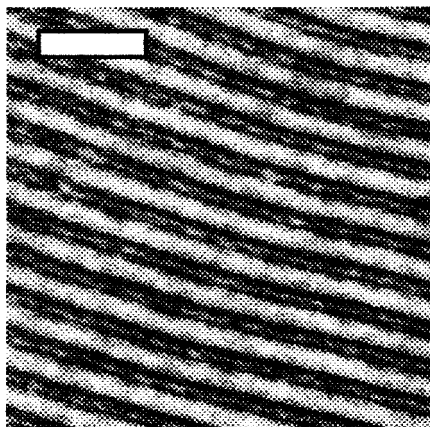
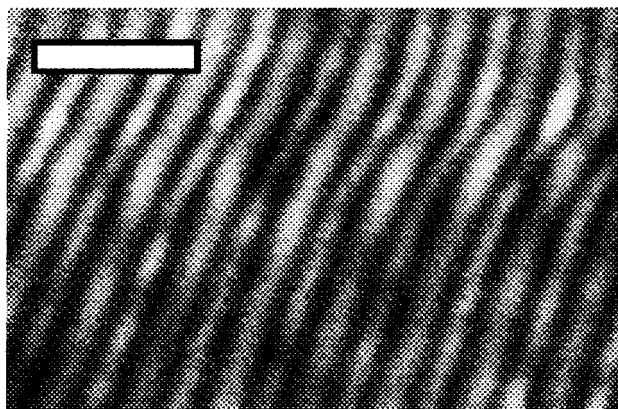
XPS line	structure	SI-46/ 11-F3	SI-46/ 11-F7	SI-46/ 11-F8
C1s	-C-C/C-H-	284.6	284.6	284.6
	-CH <sub>2</sub> -O-	286.7	286.5	286.5
	-COO-	289.8	289.5	289.6
	-CF <sub>2</sub>	291.3	291.3	291.4
	-CF <sub>3</sub>	293.5	293.5	293.5
O1s	-C=O	532.2	532.4	532.5
	-C-O	533.6	533.8	533.7
F1s	-CF	688.4	688.5	688.5

pretation of the regional F 1s and O 1s scans is straightforward. The F 1s line consists of a single symmetrical peak in all polymers. The O 1s line exhibits two components of equal areas corresponding to the two different types of oxygen atoms in the ester functional group of the perfluorinated carboxylic acid side chains.

The C 1s lines shown in Figures 4a and 5 reveal complex signals extending over an energy interval of approximately 12 eV. Although there are six chemically differently bonded carbon atoms present in our polymers, only five could be resolved clearly, and these were used for curve-fitting procedures. In contrast to the published literature<sup>14</sup> the aromatic and aliphatic carbon signals were treated as one line and were calibrated to 284.6 eV. The resulting peak assignments given in Table 2 are based on the characteristic binding energies and agree well with previously established references.<sup>14</sup> They are also representative for all other block copolymers in this study. The ratios of the different carbon moieties as obtained by curve fitting of the C 1s lines agree well with the expected ratios of the fluorinated side chain of the isoprene block. For the polymers SI-26/7-F3, -F7, -F8, and -F9 one obtains the following ratios of CF<sub>3</sub>:CF<sub>2</sub>:O-C=O:CH<sub>2</sub>-O groups for the different side chains: perfluorobutyryl (F3, expected 1:2:1:1, observed 1:1.9:0.9:1.1), perfluorooctanoyl (F7, expected 1:6:1:1, observed 1:5.9:1.2:2), perfluorononanoyl (F8, expected 1:7:1:1, observed 1:7.1:1.1:1.7), and perfluorodecanoyl (F9, expected 1:8:1:1, observed 1:8.2:1.5:1.8). Slightly higher amounts of O-C=O and CH<sub>2</sub>-O groups can be explained by the experimental errors of XPS and curve fitting procedures. In conclusion, the C 1s, O 1s, and F 1s lines reveal all of the spectroscopic details that are expected for the chemical structure of our polymers. However, only the details for the perfluorinated side chain can be detected by this means. The styrene and isoprene units only contain aromatic and aliphatic C-C and C-H moieties that do not differentiate in these spectra. However, further

**Table 3. Fluorine Amounts of Pure Block Copolymers (Sampling Depth  $\approx 100$  Å)**

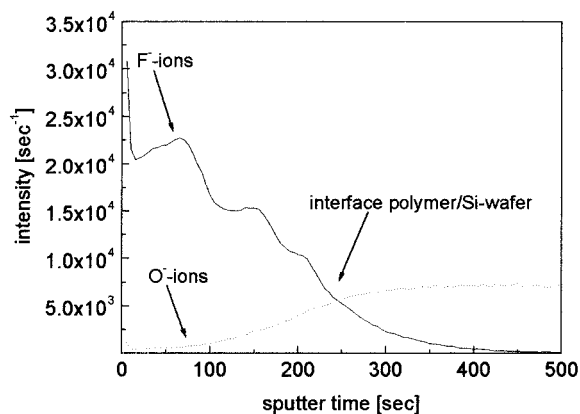
polymer	measured amount of fluorine [at. %]	calculated amount of fluorine in the bulk [at. %]	calculated amount of fluorine in isolated isoprene block [at. %]
SI-26/7-F3	37.3	18.6	38.9
SI-26/7-F7	47.2	30.2	50
SI-26/7-F8	49.9	32.1	51.5
SI-26/7-F9	49.2	33.9	52.7
SI-46/11-F3	35.2	17.5	38.9
SI-46/11-F7	54.2	28.9	50
SI-46/11-F8	56.4	31.0	51.5
SI-66/19-F3	38.9	19.3	38.9
SI-66/19-F7	55.6	31.1	50
SI-66/19-F8	55.0	33.1	51.5

**a****b****Figure 6.** TEM pictures of (a) SI-26/7-F3 and (b) SI-26/7-F7. The white scale bar represents a length of 100 nm.

information is gained from the elemental composition of the polymer surfaces.

A quantitative evaluation of the C 1s, O 1s, and F 1s peak integrals of the spectra shows a higher fluorine amount in the upper 100 Å of the polymer film with respect to the bulk composition as shown in Table 3. It is clearly seen that the measured amount of fluorine—within experimental error—equals the calculated amount in the isolated isoprene block, thus indicating that mostly the fluorinated isoprene block is present in the uppermost 100 Å of the polymer surface.

Transmission electron micrographs shown in parts a and b of Figure 6 reveal that the block copolymers phase separate, forming a lamellar structure. The lamellar period  $d_s$  of the morphology of all polymer samples is much larger than the maximum sampling depth of the

**Figure 7.** Depth profile of a 2000 Å film of SI-26/7-F7 on a silicon wafer by dynamic secondary ion mass spectrometry (dSIMS).

XPS experiment under these conditions ( $d_s = 400 \pm 20$  Å for SI-26/7-F3 and  $d_s = 435 \pm 20$  Å for SI-26/7-F7). Hence, this morphology suggests a surface excess of the fluorinated block within the sampling depth of XPS.

Evidence of the lamellar structure of the copolymer is also obtained by a depth profile with dynamic secondary ion mass spectrometry (dSIMS). A spin coated and annealed film of SI-26/7-F7 (thickness approximately 2000 Å, as measured by AFM) on a silicon wafer was investigated. The time-dependent signals of F<sup>-</sup> and O<sup>-</sup> ions are shown in Figure 7. The onset of the O<sup>-</sup> signal points to the interface of the polymer and silicon dioxide of the silicon wafer. Of particular interest are oscillations of the F<sup>-</sup> ion yield. The periodicity of the fluorine signal is consistent with the domain spacing obtained from TEM micrographs of the polymer film which can be seen as follows: We calibrate the sputter time of 245 s to reach the silicon oxid/polymer interface (at 80% of the oxygen signal) with the film thickness obtained by AFM of 2000 Å assuming a constant erosion rate. The sputter time between two maxima of about 60 s now corresponds to a depth of  $485 \pm 20$  Å. This is in fairly good agreement with the lamellae spacing of  $435 \pm 20$  Å from TEM micrographs, especially in the view of the assumption of a constant erosion rate.

Angle-dependent XPS measurements were performed on thin spin coated films of SI-26/7-F7, SI-46/11-F7, and SI-66/19-F7 at takeoff angles of  $\alpha = 90, 50, 30,$  and  $10^\circ$  that correspond to sampling depths of approximately 100, 76, 50, and 17 Å respectively as calculated for inelastic mean free paths of  $\lambda_{C1s} = 33.2$  Å and approximately 81, 62, 41, and 14 Å as calculated for  $\lambda_{F1s} = 27.1$  Å.<sup>18,19</sup> Figure 8 shows the fluorine amounts of the pure block copolymers (squares) as a function of the relative depth (relative depth = 1 corresponds to approximately 81 Å). Absolute depths were avoided as they contain uncertainties in the inelastic mean free path  $\lambda$ . The results clearly show a higher fluorine signal at shallower depths while carbon reveals the reverse effect (not shown here). The fluorine amounts of the pure isoprene blocks are 50 at. % (see Table 3) whereas the amounts at a relative depth of 0.17 are higher in all block copolymers. This suggests that the perfluorooctanoyl side chain of the isoprene block is enriched in the outermost region of the surface. However, the total fluorine amount of the isolated side chain accounts for 68% which is well above the observed amounts for the shallowest depth. Hence, only a frac-



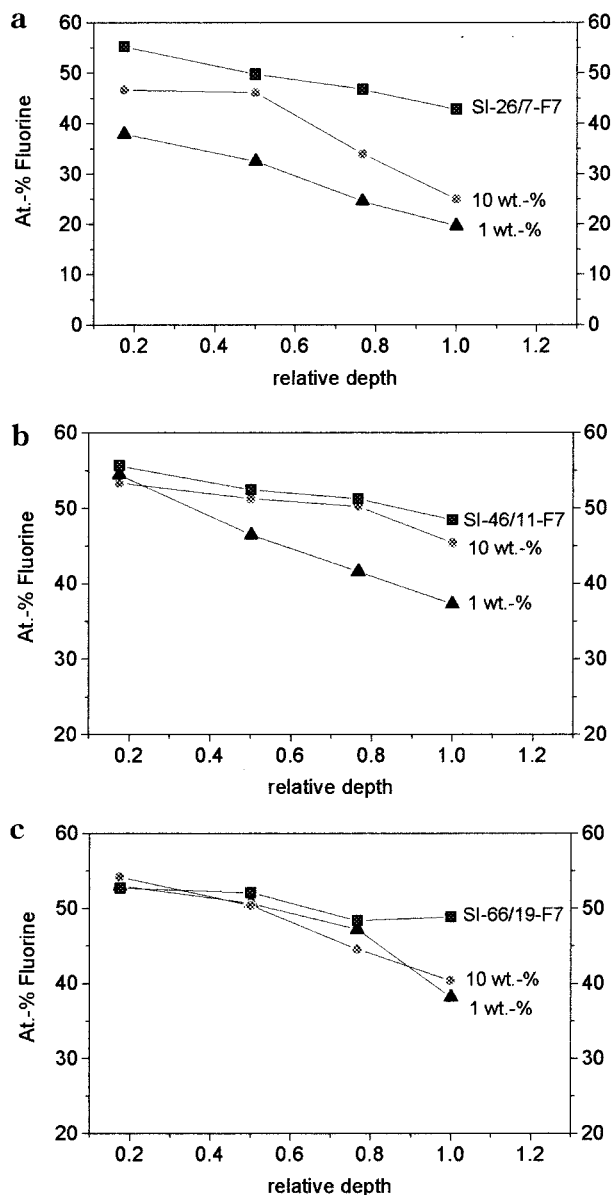


**Figure 8.** ADXPS of block copolymers and blends with polystyrene, calculated amount of fluorine in isolated isoprene block: 50 at. %, bulk fluorine amount in pure block copolymer  $\approx 30$  at. %: (a) SI-26/7-F7 and blends with PS 72; (b) SI-46/11-F7 and blends with PS 72; (c) SI-66/19-F7 and blends with PS 72.

tional surface excess of the side chain is present in the outermost surface region. However, the entire depth investigated by XPS consists of the fluorinated isoprene block of the copolymer.

The observation of a surface enrichment of the perfluorinated side chains are in qualitative agreement with prior observations<sup>20</sup> in the investigation of styrene-isoprene block copolymers with semifluorinated side chains  $((-\text{CH}_2)_m-\text{C}_n\text{F}_{2n+1})$  having hydrocarbon spacer of  $m \leq 8$  methylene groups between the fluorinated side chains and the isoprene unit. Small-angle X-ray scattering of the lamellar block copolymer showed that the fluorinated isoprene block at the surface was structured such that the uppermost layer consists of semifluorinated side chains perpendicular to the surface. Within the lamella—below the uppermost perpendicular layer—the side chains are structured parallel to the surface, forming smectic layers. Such highly ordered structures are formed due to the presence of flexible hydrocarbon

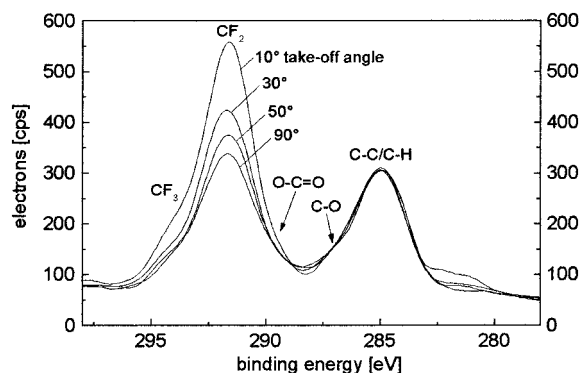


**Figure 9.** ADXPS C 1s regional scan of SI-46/11-F7.

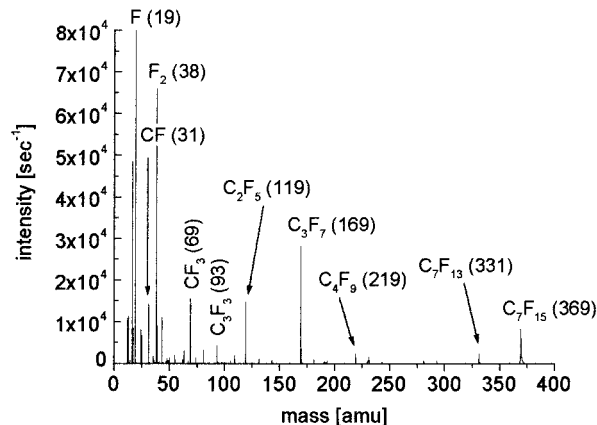


**Figure 10.** Static secondary ion mass spectrum (sSIMS) of SI-26/7-F7.

spacers.<sup>13</sup> As a result, our much more rigid perfluorinated side chains are not expected to yield such highly ordered structures. Hence, the less ordered structure of the side chains apparently only leads to a fractional surface excess within the isoprene containing top layer of the surface.

Further evidence for the enrichment of the side chain within the isoprene block containing—uppermost layer is derived from ADXPS in Figure 9 for the SI-46/11-F7 block copolymer. If the spectra are normalized to their C-C/C-H peak heights, one clearly sees the higher amount of CF<sub>2</sub> and CF<sub>3</sub> moieties relative to the non-fluorine-containing carbon atoms as the sampling depth decreases.

Finally, supporting evidence of the structural results comes from static time-of-flight secondary ion mass spectrometry (ToF-SIMS) owing a sampling depth of approximately 10 Å. Because of the fact that fluorine containing polymers have very high secondary ion yields, both for positive and negative secondary ions, this technique is of particular value for structural characterization. A negative ion mass spectrum obtained from SI-26/7-F7 is shown in Figure 10. Beside the signals of (F)<sup>-</sup> (19 amu), (F<sub>2</sub>)<sup>-</sup> (38 amu) and (CF)<sup>-</sup> (31 amu) ions one observes a series of peaks of high intensity that differ by 50 amu. These ions are supposed to be (CF<sub>2</sub>)<sub>n</sub>CF<sub>3</sub><sup>-</sup>, where  $m/z = 69 + 50n$  ( $n = 0, 1, 2, 3, \dots$ ) and originate from the perfluorocarbon side chains of the polymer. All other signals of fluorocarbon fragments represent masses that differ by 19 or 12 amu, presumably from the series mentioned above by additional C-C and C-F bond cleavage between the perfluorocarbons. Peaks that are known to be characteristic of polystyrene<sup>21</sup> are only detectable with very

**Table 4. Advancing, Receding, and Static Contact Angles of Water**

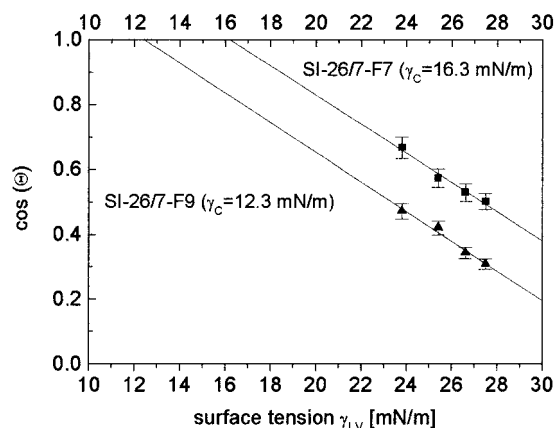
polymer	advancing	receding	static	hysteresis
	contact angle $\theta_{adv}$ (deg)	contact angle $\theta_{reced}$ (deg)	contact angle $\theta$ (deg)	$\theta_{adv} - \theta_{reced}$ (deg)
SI-26/7-F3	99	76	95	23
SI-26/7-F7	113	88	107	25
SI-26/7-F8	115	91	113	24
SI-26/7-F9	122	102	119	20
SI-46/11-F3	102	82	100	20
SI-46/11-F7	112	90	111	22
SI-46/11-F8	117	93	113	24
SI-66/19-F3	103	82	99	21
SI-66/19-F7	113	90	109	23
SI-66/19-F8	114	92	110	22
SI-59/10-F1	102	67	80	35
SI-59/10-F3	106	87	100	19
SI-59/10-F7	117	94	105	23
SI-19/18-F1	104	68	82	36
SI-19/18-F3	109	90	99	19
SI-19/18-F7	121	96	106	25
polystyrene	89	78		11
polytetrafluoroethylene	110	105		5

low intensities, e.g., mass  $(C_6H_5)^+$  77 amu or  $(C_7H_7)^+$  91 amu, thus proving further evidence for the surface enrichment of the fluorinated side chains at the surface.

The molecular composition reported here is consistent with contact angle measurements of thin polymer films spin coated on polished silicon wafers. All samples except SI-26/7-F3 exhibit advancing contact angles against water that are larger than  $100^\circ$  as shown in Table 4. More detailed information about the surface tension and surface composition is revealed from contact angles of nonpolar liquids. These allow the determination of the critical surface tension according to Zisman.<sup>22</sup> The contact angles against hydrocarbon oils reveal oleophobicity for SI-26/7-F8 and SI-26/7-F9 that comes close to the highest contact angle values as measured by Zisman et al. for surfaces covered by  $CF_3$  groups ( $75$ – $78^\circ$ /hexadecane).<sup>22</sup> They found that a monolayer of a uniform hexagonally close packed array of perfluorocarboxylic acids with a surface consisting purely of  $CF_3$  groups yields a critical surface tension ( $\gamma_C$ ) of 6 mN/m.<sup>23</sup> According to Zisman even surfaces with hexadecane contact angles around  $54^\circ$  are considered to be highly oleophobic. The smaller the value of  $\gamma_C$ , the more hydrophobic and oleophobic is the sample surface as easily derived from the definition of the critical surface tension, where the value of  $\gamma_C$  marks the limit of complete wetting of the surface ( $\cos \theta = 1$  for contact angle  $\theta = 0^\circ$ ; i.e., liquids with surface tensions  $\gamma_{LV}$  smaller than the  $\gamma_C$  will spread on the polymer film surface and wet it completely).

In the case of poly(tetrafluoroethylene) (Teflon), where the surface nearly completely consists of  $CF_2$  groups, the critical surface tension rises to a value of 15 mN/m.<sup>24</sup> As the  $\gamma_C$  value of all polymers (annealed for 3 h at  $140^\circ C$ ) shows a clear dependence on the length of the perfluorinated side chain and is equal to (SI-26/7-F8) or even smaller than (SI-26/7-F9) that of PTFE within the error range of extrapolation ( $\pm 1$  mN/m), as shown in Table 5 and Figure 11, we can conclude that the  $\gamma_C$  values indicate that the surfaces of our polymer films are nearly exclusively occupied by  $CF_3$  and  $CF_2$  groups.

The hysteresis between the advancing and the receding contact angles are on the order of  $19$ – $36^\circ$  (see Table 4), which is substantially larger in comparison to the mentioned semifluorinated side chains.<sup>13,20</sup> They exhibit

**Figure 11.** Zisman plot of fluorinated side chain block copolymers SI-26/7-F7 and SI-26/7-F9.**Table 5. Contact Angles and Critical Surface Tension of SI-26/7 Block Copolymers**

polymer	hexadecane $\gamma_{LV} = 27.5$ mN/m	tetradecane $\gamma_{LV} = 26.6$ mN/m	dodecane $\gamma_{LV} = 25.4$ mN/m	decane $\gamma_{LV} = 23.8$ mN/m	critical surface tension $\gamma_C$ [mN/m]
SI-26/7-F3	56	47	45	42	18.4
SI-26/7-F7	60	58	55	48	16.3
SI-26/7-F8	74	70	64	61	15.2
SI-26/7-F9	72	70	65	62	12.3

**Table 6. Fluorine Amounts of Pure Block Copolymers and Blends with Polystyrene PS 72 (10 wt % and 1 wt % Fluorinated Block Copolymers in PS Matrix) (Sampling Depth  $\approx 100$  Å)**

polymer	fluorine amount				
	pure diblock	10 wt %		1 wt %	
		200 nm thick film	5 $\mu m$ thick film	200 nm thick film	5 $\mu m$ thick film
SI-26/7-F3	37.3	22.7	30.3	n/a	14.4
SI-26/7-F7	47.2	28.3	42.8	13.1	33.1
SI-46/11-F7	54.2	24.8	43.1	12.8	45.2
SI-66/19-F7	55.6	30	43.6	14.8	43.8

a hysteresis of  $10$ – $15^\circ$ . The difference is likely due to the more homogeneous surface structures in the semifluorinated side chains as a consequence of the flexible hydrocarbon spacer leading to highly ordered structures already mentioned above. Additional support is obtained from the critical surface tension. Whereas the surfaces with spacers have critical surface tensions of  $8$ – $10$  mN/m,<sup>13</sup> our perfluorinated side chains exhibit higher values on the order of  $12$ – $20$  mN/m depending on the length of the side chain. Longer side chains have smaller critical surface tensions. Finally, it is underlined that the surface tensions and contact angles reported here are in good agreement with similar poly(styrene-*b*-butadiene) copolymers having perfluorooctanic ester side chains previously reported by Antonietti et al.<sup>25</sup>

**Polymer Blends.** To study the segregation phenomena in a homopolymer that corresponds to the non-fluorine-containing block of the copolymer, blends containing 10 and 1 wt % block copolymer in polystyrene ( $M_w = 72$  kg/mol; PS 72, Polymer Standard Service, Mainz, Germany) were prepared and investigated. The surface composition of the uppermost  $\approx 100$  Å of differently prepared films on silicon wafers was determined by XPS as shown in Table 6. One notices large differences in the fluorine surface enrichment between thin spin-coated (200 nm) and cast thick films (5  $\mu m$ ). The latter consist of fluorine amounts two to three times



higher than the spin-coated samples. The depletion in the spin-coated films does not even change significantly upon annealing at 140 °C for several hours. In addition, the fluorine surface enrichment of the 5  $\mu\text{m}$  thick films shows values nearly as high as in the pure block copolymer films within experimental error. This is a result of the strong surface segregation of our fluorinated block copolymers due to the low surface energy of the perfluorocarbon side chain. Only small amounts of 1 wt % of the fluorinated polymer are sufficient to obtain a surface composition similar to that of the pure copolymer film. This is in qualitative agreement to the literature,<sup>5</sup> where the segregation isotherm at 160 °C for a similar diblock copolymer of deuterated styrene and isoprene with a perfluorinated F3 side chain (in our notation d-SI-29/2-F3) reveals a surface excess that equals the plateau value at a bulk volume fraction of 0.02. The differences between the films prepared by the two preparation methods can be explained as follows. Slow evaporation of the solvent allows a longer segregation time of the fluorinated block copolymer in a mixture of a lower viscosity compared to spin coating. Here, the viscosity of the polymer solution quickly rises to high near-bulk values, thus reducing the chain mobility. It is important to note that the pure block copolymer samples did not show any dependence of the fluorine surface enrichment on the film thickness. The results also show that for thin (200 nm) films containing blends of SI-26/7-F7, SI-46/11-F7, and SI-66/19-F7 with PS 72 there is a decrease in the fluorine surface composition by decreasing the overall fluorine weight percentage in the bulk as shown in Table 6, which is not observed for thick (5  $\mu\text{m}$ ) films and can also be explained by the differences in viscosity during film preparation, as mentioned above.

ADXPS was performed for blends of the copolymer with perfluorooctanoyl as a side chain in PS 72 (10 and 1 wt % blends). At small takeoff angles the fluorine surface amounts are much larger than expected for a random bulk morphology as shown in Figure 8. In particular, in the case of SI-46/11-F7 and SI-66/19-F7, the values at small angles were as high as those of the pure block copolymers. The blends of SI-46/11-F7 and SI-66/19-F7 with polystyrene show higher fluorine enrichments than those of SI-26/7-F7, especially at small angles. This suggests that SI-46/11-F7 and SI-66/19-F7 have the greater ability to phase separate and to form larger fluorocarbon domains at the surface due to the longer fluorinated isoprene blocks.

#### Thermal Cleavage of Fluorinated Side Chains.

The thermal stability of the block copolymers was characterized using thermogravimetric analysis (TGA) and thermal desorption mass spectrometry (TDMS). Figure 12 shows TGA scans of SI-26/7-F3 and -F7 that clearly reveal a two-step degradation process. In particular, the first derivative of the relative weight vs temperature shows two distinct minima, the first one being at a temperature around 340 °C with a second minimum at approximately 420 °C. The degradation process according to the first minimum can be well understood by the known reaction of an ester pyrolysis. Scheme 3 depicts the possible reaction and its suggested mechanism corresponding to a retro-ene reaction.<sup>26</sup> The weight loss of the first degradation step correlates well with the overall loss expected for the quantitative cleavage of the fluorinated carboxylic acid side chains as shown in Table 7. Furthermore, it can be seen that the temperature of the first degradation step does not depend on the block copolymer composition. The second

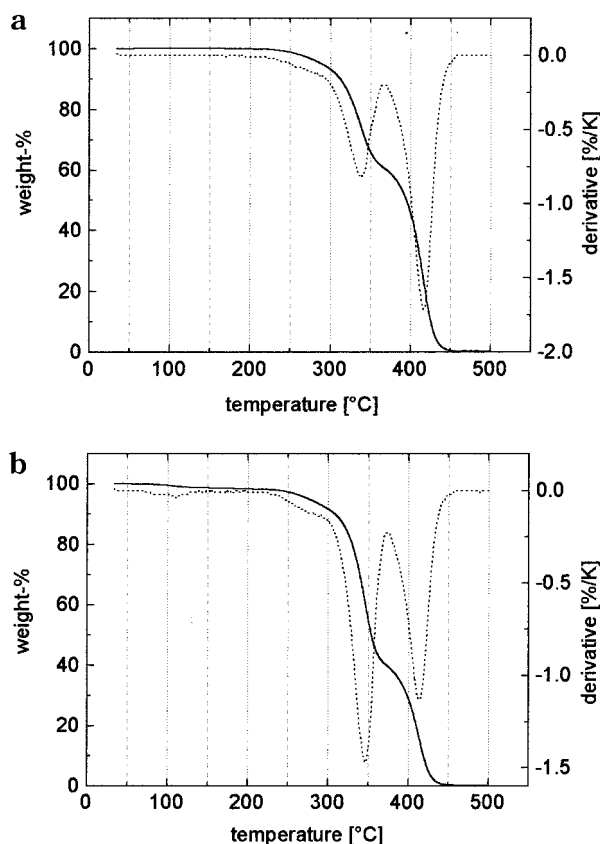


**Figure 12.** TGA data of (a) SI-26/7-F3 and (b) SI-26/7-F7.

#### Scheme 3. Proposed Ester Pyrolysis Reaction and Mechanism

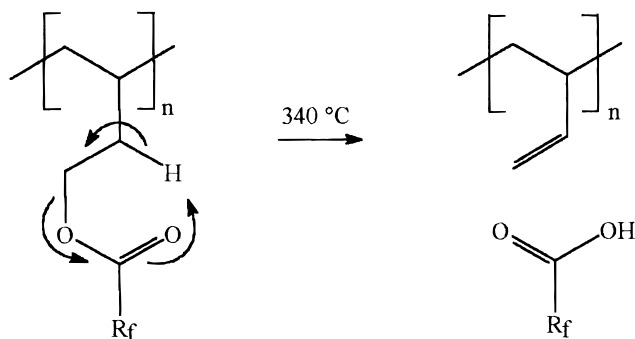


**Table 7.** Thermogravimetric Analysis (TGA) of Fluorinated Side Chain Block Copolymers

polymer	loss of mass (%)		degradation step (°C)	
	calculated	experimental	first	second
SI-59/10-F1	17	17	335	419
SI-59/10-F3	30	30	341	420
SI-59/10-F7	46	47	347	420
SI-59/10-H8F10	55	no evaluation possible	414	423
SI-59/10-H1	11	100	398	
SI-19/18-F1	39	41	336	416
SI-19/18-F3	56	61	340	419
SI-19/18-F7	72	75	345	419
SI-26/7-F3	40	40	338	417
SI-26/7-F7	56	60	347	414
SI-26/7-F8	59	78	345	394
SI-26/7-F9	61	53	348	403

degradation step occurs at a temperature of approximately 80 K above the first step. It is assumed to be the decomposition of the poly(styrene-*b*-isoprene) block

copolymer, the solid polymeric reaction product of the ester pyrolysis.

The reaction scheme is supported by an analysis with *in situ* infrared spectroscopy of a copolymer film during the thermal treatment. Up to a temperature of 340 °C, only the intensity of signals that correspond to the ester ( $\tilde{\nu}(\text{C}=\text{O})$  at 1786  $\text{cm}^{-1}$ ,  $\tilde{\nu}_{\text{S/AS}}(\text{CF}_2)$  at 1140–1240  $\text{cm}^{-1}$ , and  $\tilde{\nu}_{\text{S/AS}}(\text{CF}_3)$  at 1169/1227  $\text{cm}^{-1}$ ) are decreasing while the intensity of the signal corresponding to the vinyl group ( $\tilde{\nu}(\text{C}=\text{C})$  at 886 and 996  $\text{cm}^{-1}$ ) increases. Subsequent XPS analysis of the film that was heated to 340 °C does not show any fluorine. Further results of the thermally treated films will be presented in another publication.<sup>27</sup>

The two-step process with a temperature difference of 80 K is only observed for a side chain consisting of a perfluorinated carboxylic acid. The same polymer backbone with semifluorinated carboxylic acid side chains (SI-59/10-H8F10: 8 methylene units as spacer between fluorinated chain and ester group; the polymer was taken from a previous publication<sup>13</sup>) does not show two separate degradation steps as seen from the temperatures in Table 7. Here, the first degradation temperature is about 70 K higher compared to the perfluorinated ester side chain. A nonfluorinated carboxylic acid side chain like an acetic acid ester (SI-59/10-H1; see previous publication<sup>13</sup>) shows a decomposition at a temperature that lies between the two degradation minima of the perfluorinated acid side chain block copolymers. The observations can be well understood assuming the above-mentioned classical pyrolytic reaction. For a monomeric acetic ester one gets a pyrolysis temperature of 400–500 °C from the literature.<sup>28</sup> The temperature of the ester cleavage of the perfluorinated groups is expected to be lower due to the activation of the ester bond by the electron-withdrawing effect of the highly electronegative fluorine substituents.

To further support the conclusion of the selective cleavage of the perfluorocarboxylic acid side chains, thermal desorption mass spectrometry (TDMS) was employed. Here, fragments originating from the fluorocarbon side chain can be well distinguished from those of the hydrocarbon backbone. Fluorocarbon fragments are observed by a homologous series following the formula  $\text{C}_n\text{F}_{2n+1}^+$  and  $\text{C}_n\text{F}_{2n}^+$  ( $\text{CF}_3^+/69$  amu,  $\text{C}_2\text{F}_5^+/119$  amu,  $\text{C}_3\text{F}_7^+/169$  amu,  $\text{CF}_2^+/50$  amu,  $\text{C}_2\text{F}_4^+/100$  amu for the heptafluorobutyl side chain and, additionally,  $\text{C}_5\text{F}_{11}^+/269$  amu for the perfluorooctanoyl side chain). For the hydrocarbon backbone, the most intense fragments observed were the highly stable aromatic ions:  $\text{C}_6\text{H}_5^+/77$  amu,  $\text{C}_6\text{H}_6^+/78$  amu,  $\text{C}_7\text{H}_7^+/91$  amu, and  $\text{C}_8\text{H}_8^+/104$  amu. The relative yields of these ions were monitored during heating.

A TDMS spectrum of SI-26/7-F7 is shown in Figure 13a. Two groups of signals can be distinguished, representing fragments originating from the fluorocarbon side chain and the hydrocarbon backbone. As summarized in Table 8, the decomposition temperatures match well with the temperatures observed in TGA (see Table 7). Slightly higher temperatures in TDMS can be explained by differences in the surface area covered by the polymer film between different samples. For a true thermal desorption situation in TDMS the desorption temperature is proportional to the ratio coverage/area (e.g., one finds higher desorption temperatures for a higher coverage/area<sup>29</sup>). However, the difference between the appearance of CF and CH fragments remains constant at around 80 K.

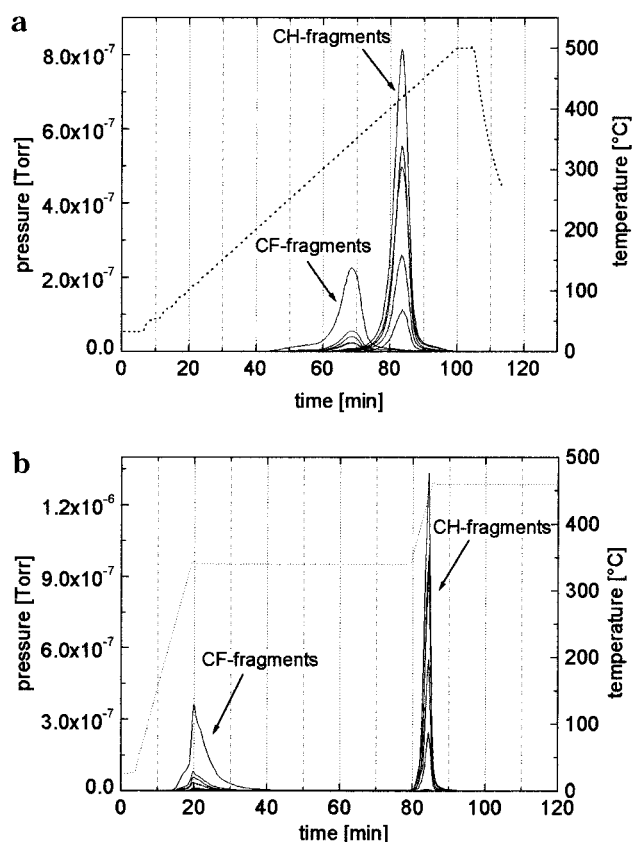


**Figure 13.** TDMS spectra of SI-26/7-F7 (a) continuous heating and (b) two-step heating.

**Table 8.** TDMS Data of Fluorinated Side Chain Block Copolymers

polymer	temperature at peak I (°C)	temperature at peak II (°C)
SI-26/7-F3	348	450
SI-26/7-F7	345	420
SI-59/10-F3	340	414
SI-59/10-F7	354	431

Additionally, using a two-step temperature experiment, it can be shown that at a temperature of 340 °C only decomposition of the fluorocarbon side chain is observed. Figure 13b shows a scan of SI-26/7-F7 where the two decomposition processes are separated by holding an intermediate temperature of 340 °C. Clearly, the two decomposition processes are fully separated. Finally, XPS measurements of thin film samples of our polymers (after heating to 340 °C for 15 min in a vacuum oven) revealed that no residual fluorocarbon fragments could be detected at the surface of the visually unaltered polymer film.

The reported results allow the conclusion that the fluorinated side chain can be cleaved off selectively and that the correlation between the weight loss during TGA experiments and the calculated overall weight of the side chains is not coincidental. A mechanism as shown in Scheme 3 further suggests the restoration of the vinyl groups through thermally induced ester bond cleavage. However, the presence of residual amounts of oxygen during thermal cleavage might lead to some cross-linking of the isoprene block.

The thermal cleavage of the fluorinated side chains obviously leads to a striking reduction of the contact angle. For example, films of SI-26/7-F9 exhibit an advancing water contact angle of 122° (see Table 4) prior to heating, which is reduced to 87° after thermal

cleavage at 340 °C. Similar results leading to advancing contact angles <90° are observed for all other polymers reported here.

Possible applications of the block copolymers reported here are evidently related to the high hydrophobicity combined with the selective thermal cleavage. Since the thermal treatment can be carried out locally, surfaces with patterns of hydrophobic and hydrophilic areas seem possible. These are the basis for printing processes with aqueous inks. Moreover, the defined reaction product after cleavage offers a scheme that allows chemical derivatization thus suggesting to change the surface chemistry and subsequently its surface properties in a very controlled manner. In combination with laterally resolved thermal treatment this may be used as a new technique of laterally structuring and functionalizing polymer surfaces. Work in this area is still in progress and will be presented and discussed in a separate paper.

### Conclusion

Monodisperse poly(styrene-*b*-isoprene[*-g*-perfluoroacyl]) block copolymers synthesized in this paper reveal extraordinary surface properties. Films of the pure blocks and their 10 and 1 wt % blends with polystyrene exhibit high fluorine enrichments at the surface that originate from strong surface segregation of the fluorinated isoprene block. Surface and bulk morphologies of the pure block copolymers consist of lamellae with periods of the order of 430 Å. As obtained from XPS, the uppermost 100 Å nearly completely consist of the isoprene block. In addition, a fractional surface excess of the fluorinated side chain within the isoprene layer is observed. However, the structures appear less ordered compared to semifluorinated side chains having up to eight methylene group spacers.

The perfluorinated side chains can be selectively thermally cleaved by heating the polymer to a temperature of approximately 340 °C. The weight loss during thermogravimetric analysis and fragments detected by mass spectrometry as well as XPS measurements of the polymer surfaces after thermal treatment under vacuum conditions showed that the fluorinated side chain can be cleaved without degradation of the polymer backbone. The polymer surfaces are highly hydrophobic and exhibit advancing water contact angles of up to 122° for perfluorodecanoyl side chains. Upon heating and selective cleavage, the advancing contact angle is lowered to <90°.

The surface excess of the fluorocarbon side chains in combination with the selective thermal cleavage without damaging the polymer backbone has potential for creating hydro- and oleophobic patterns. The chemically defined ester cleavage may lead to patterned surface functionalities upon chemical surface derivatization.

**Acknowledgment.** We gratefully acknowledge the support by M. Voetz, S. Greb, W. Loyen, and D. Rühle during the XPS and SIMS and contact angle measure-

ments. A.B. would like to thank G. Mannebach for teaching him anionic polymerization, T. Herweg for the invaluable help with the TDMS measurements and B. A. Wolf (Mainz, Germany) for inspiring discussions and his support during completion of this work. C.K.O. is grateful for partial support for this work from the Office of Naval Research.

### References and Notes

- (1) Pittman, A. G. In *Fluoropolymers*; Wall, L. A., Ed.; Wiley: New York, 1972, Vol. 25.
- (2) Scheirs, J., Ed. *Modern Fluoropolymers*; Wiley: Chichester, England, 1997.
- (3) Katano, Y.; Tomono, H.; Nakajima, T. *Macromolecules* **1994**, *27*, 2342.
- (4) Hopken, J.; Möller, M. *Macromolecules* **1992**, *25*, 1461.
- (5) Iyengar, D. R.; Perutz, S. M.; Dai, C. A.; Ober, C. K.; Kramer, E. J. *Macromolecules* **1996**, *29*, 1229.
- (6) Shull, K. R.; Kramer, E. J. *Macromolecules* **1990**, *23*, 4769.
- (7) Dai, K. H.; Shull, K. R.; Kramer, E. J. *Macromolecules* **1992**, *25*, 220.
- (8) DeForest, W. S. *Photoresistant Materials and Processes*; McGraw-Hill: New York, 1975.
- (9) Filler, R.; O'Brien, J. F.; Fenner, J. V.; Hauptschein, M. *Chem. Soc.* **1953**, *75*, 968.
- (10) Brown, H. C.; Knights, E. F.; Scouten, C. G.; *J. Am. Chem. Soc.* **1974**, *96*, 7765.
- (11) Mao, G. M.; Wang, J. W.; Clingman, S. R.; Ober, C. K.; Chen, J. T.; Thomas, E. L. *Macromolecules* **1997**, *30*, 2556.
- (12) Chung, T. C.; Raate, M.; Berluche, R. E.; Schulz, D. N.; *Macromolecules* **1988**, *21*, 1903.
- (13) Wang, J.; Mao, G.; Kramer, E. J.; Ober, C. K. *Macromolecules* **1997**, *30*, 1906.
- (14) Beamson, G.; Briggs, D. *High Resolution XPS of Organic Polymers, The Scientia ESCA 300 Database*; Wiley: New York, 1992.
- (15) Powell, C. J. *J. Electron Spectrosc. Relat. Phenom.* **1988**, *47*, 197.
- (16) Seah, M. P.; Dench, W. A. *Surf. Interface Anal.* **1979**, *1*, 2.
- (17) Jones, R. A.; Kramer, E. J.; *Polymer* **1993**, *34*, 115.
- (18) Kassiss, C. M.; Steehler, J. K.; Betts, D. E.; Guan, Z.; Romack, T. J.; DeSimone, J. M.; Linton, R. W. *Macromolecules* **1996**, *29*, 3248.
- (19) Ebel, H.; Ebel, M. F.; Baldauf, P.; Jablonski, A. *Surf. Interface Anal.* **1978**, *12*, 172.
- (20) Muthukumar, M.; Ober, C. K.; Thomas, E. L. *Science* **1997**, *277*, 1225.
- (21) Vickerman, J. C.; Briggs, D.; Leggett, G. J.; Hagenhoff, B.; Chilkoti, A.; Bryan, S.; McKeown, P. J. *The Wiley Static SIMS Library*; Wiley: Chichester, England, 1996.
- (22) Shafrin, E. G.; Zisman, W. A. *Contact Angle and Wettability*; Advances in Chemistry Series 43; American Chemical Society: Washington, DC, 1964; p 151.
- (23) Hare, E. F.; Shafrin, E. G.; Zisman, W. A. *J. Colloid Sci.* **1954**, *58*, 236.
- (24) Ellison, A. H.; Fox, H. W.; Zisman, W. A. *J. Phys. Chem.* **1953**, *57*, 622.
- (25) Antonietti, M.; Förster, S.; Micha, M. A.; Oestreich, S. *Acta Polym.* **1997**, *48*, 262.
- (26) Fleming, I. *Frontier orbitals and organic chemical reactions*; Wiley: London, 1976.
- (27) Böker, A.; Reihls, K.; Ober, C. K. To be submitted to *Macromolecules*.
- (28) Burns, R.; Jones, D. T.; Ritchie, P. D. *J. Chem. Soc.* **1935**, 400.
- (29) Redhead, P. A. *Vacuum* **1962**, *12*, 203.

MA990828+